AD-A050 323 BOEING AEROSPACE CO SEATTLE WASH F/G 20/4
FLOW FIELD MATCHING.(U)
JAN 78 L J DICKSON, K D LEE, A W CHEN N00014-76-C-0931
UNCLASSIFIED D180-24040-1 NL

| OF |
AD
A050323

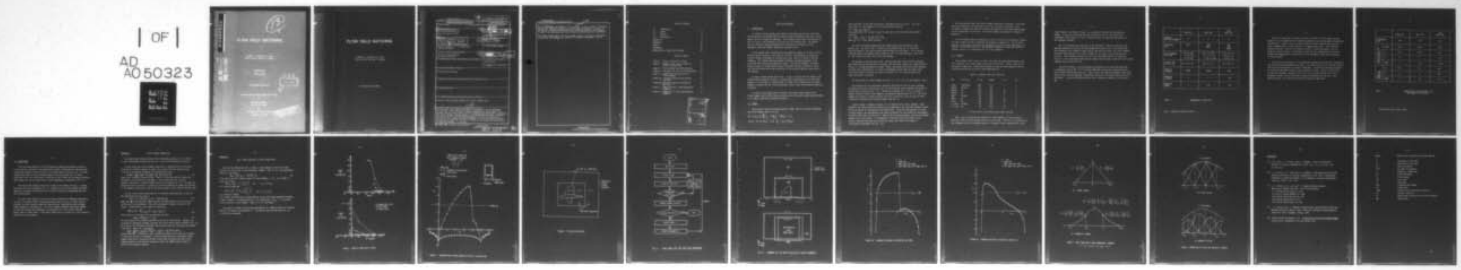

END
DATE
FILMED
3-78
DDC

13

FLOW FIELD MATCHING

Lawrence J. Dickson, Ki D. Lee,
Allen M. Chen, and Paul E. Rubbert

D-180-24040-1
February 1976

Distribution unlimited

Prepared under Contract N00014-76-C-0831
by
The Boeing Company
Seattle, WA 98124
for
the Office of Naval Research
Arlington, VA 22217

FLOW FIELD MATCHING

Lawrence J. Dickson, Ki D. Lee,
Allen W. Chen, and Paul E. Rubbert

Unclassified
SECURITY CLASSIFICATION OF THIS PAGE (When Data Entered)

(14) D180-24040-1

REPORT DOCUMENTATION PAGE

READ INSTRUCTIONS BEFORE COMPLETING FORM

1. REPORT NUMBER
2. GOVT ACCESSION NO.
3. RECIPIENT'S CATALOG NUMBER (rec't.)

(6) TITLE (and Subtitle): Flow Field Matching.

(9) Final (May [redacted]76 - Jan. [redacted]78)

5. PERFORMING ORG. REPORT NUMBER: D-180-24040-1

(10) 7. AUTHOR(s): Lawrence J./Dickson, Ki D./Lee, Allen W./Chen, Paul E./Rubbert

(15) 8. CONTRACT OR GRANT NUMBER(s): N0014-76-C-0931

9. PERFORMING ORGANIZATION NAME AND ADDRESS
Boeing Aerospace Co., P. O. Box 3707
Seattle, WA 98124

10. PROGRAM ELEMENT, PROJECT, TASK AREA & WORK UNIT NUMBERS

11. CONTROLLING OFFICE NAME AND ADDRESS
Office of Naval Research
Arlington, VA 22217

(11) 12. REPORT DATE: Jan [redacted]78

(12) 26 p.

13. NUMBER OF PAGES: 21

14. MONITORING AGENCY NAME & ADDRESS (if different from Controlling Office)

15. SECURITY CLASS. (of this report): Unclassified

15a. DECLASSIFICATION/DOWNGRADING SCHEDULE

16. DISTRIBUTION STATEMENT (of this Report)
Distribution Unlimited

17. DISTRIBUTION STATEMENT (of the abstract entered in Block 20, if different from Report)

18. SUPPLEMENTARY NOTES

19. KEY WORDS (Continue on reverse side if necessary and identify by block number)
Transonic flow, matching boundary, far field, middle field

(is used)

20. ABSTRACT (Continue on reverse side if necessary and identify by block number)
In a transonic flow problem with subsonic freestream in an untransformed infinite flow field, the outer boundary conditions are hard to apply. By assuming that the flow outside an artificial matching boundary is subcritical and linear, we use a Prandtl-Glauert solution (generated by panels of Green's function integrals along the matching boundary) in the far field, while solving the near field by finite differences. The two solutions are joined iteratively by requiring continuity of potential and normal derivative across the matching boundary. → over

DD FORM 1 JAN 73 1473 EDITION OF 1 NOV 65 IS OBSOLETE

Unclassified
SECURITY CLASSIFICATION OF THIS PAGE (When Data Entered)

059 610

We also examine two refinements of this method. In one, a locally linearized second-order far field solution (a Poisson equation solution) is used. In the second, a middle field inhabited by large rectangular finite elements is used in the area where the flow is highly nonlinear but still subcritical.

This report details only the finite element results, the earlier ones having already been published in the scientific literature (references 1 and 2).

Table of Contents

I.	Introduction	1
II.	Theory	1
III.	Results	3
IV.	Conclusions	8
Appendix A		9
Appendix B		10
Figures		11
References		20
Abbreviations, Symbols and Acronyms		21

Table of Figures

Figure 1 - Error as function of effort	11
Figure 2 - Boundary meets lower surface of airfoil in mixed flow	12
Figure 3 - Finite element mid-field matching	13
Figure 4 - Flow Chart for the far-field matching	14
Figure 5 - Example of 3-D mid-field with finite elements	15
Figure 6A - Chordwise pressure distribution (at root)	16
Figure 6B- Chordwise pressure distribution (near tip)	17
Figure 7 - Shape functions in one-dimensional elements	18
Figure 8 - Comparison of linear and Quadratic elements	19

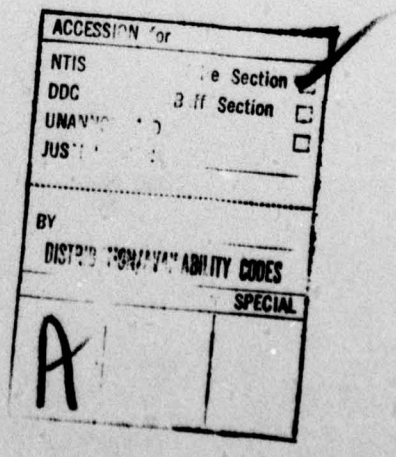

FLOW FIELD MATCHING

I. INTRODUCTION

In transonic flow problems with subsonic freestream and infinite flow field, discretized solution methods which by nature solve the equations only over a finite domain are not in themselves adequate. The influence on the near field solution of the "far field", which extends to infinity, must be accounted for. The present work has explored a matching method which has proved to be superior to the asymptotic expansion commonly employed to accomplish this.

In the problem under consideration, the equations reduce to a linear, elliptic Prandtl-Glauert equation in the limit at infinity. That equation is soluble on infinite regions by methods of superposition using "panels" of Green's function integrals. The simplest matching method introduces a matching boundary in the flow field well outside the supersonic region. Outside the boundary, a Prandtl-Glauert solution is found, while inside a nonlinear transonic solution is found such that both value and normal derivative of the velocity potential match across the boundary.

Two more refined methods were tried. In one, a Poisson term was added to the Prandtl-Glauert equation to make it a second-order approximation to the nonlinear equation. In the other, a "middle field" of large finite elements was introduced between the panels and the (finite difference) inner field, with matching conditions as before.

In order to avoid duplication of effort, the present report details the finite element results while only outlining results that have already been published in our papers and previous quarterly reports.

II. THEORY

The transonic small disturbance equation (TSDE) used in the finite difference and finite element areas is in 3D,

$$(1)\quad \left(K\phi_x - K_\gamma \frac{\phi_x^2}{2}\right)_x + (\phi_y)_y + (\phi_z)_z = 0,$$

where $K = 1 - M_\infty^2$ and $K_\gamma = (\gamma+1)M_\infty^2$.

The 2D equation is the same except the y- derivative term is missing. The first order (FO) far field equation is the Prandtl-Glauert equation

(2) $K\phi_{xx} + \phi_{yy} + \phi_{zz} = 0$.

The second order (SO) Poisson correction term used in the 2D second order method satisfies

(3) $K\Psi_{xx} + \Psi_{zz} = K_\gamma \frac{\partial}{\partial x}(\phi_x^{(1)})^2/2$,

where $\phi^{(1)}$ is a first order solution.

The finite difference method used was conservative over-relaxation of the Murman type. The outer flow is solved by source panels (see ref. 4) along the matching boundary, the solution being updated every 10 to 80 sweeps. In the second-order 2D method, the equation being solved for Ψ is linearized about a new value of $\phi^{(1)}$ about once every five first order updates.

Two methods of matching were tried: Revising the outer flow to partly eliminate the normal derivative discontinuity between inner and outer regions (an "underelaxation" factor of .5 being theoretically optimal here), and adding sufficient source strength to cancel this discontinuity if it were superimposed on both inner and outer flows. The latter method is simpler and easier to justify (ref. 1), and both seem to be about equivalent in practice.

For more details on these methods see refs. 1, 2, 3.1, 3.2, 3.3. and Figures 1 and 2.

The extension of the second-order method to 3D proved to involve really unwieldy influence-coefficient calculations, and its stability was called somewhat into question by the later 2D results (ref. 3.3). Therefore we decided (ref. 3.4) to introduce a middle field with large finite elements satisfying an approximation to (1). The finite element (FE) region is highly nonlinear but still subcritical, and the usual elliptic variational approaches are therefore usable (see ref. 5).

Figure 3 shows a schematic example of a 3-D midfield with finite elements. Both potential and normal derivative continuity are enforced on the interface boundary between FD and FE regions by overlapping by one mesh width. Since the same equation is solved in both regions, the overlapping gives enough resolution for the continuity requirements. Dirichlet conditions are used on all sides of the FE region boundary, and the overlapping updates every cycle result in convergence of the normal derivative jump to zero. Figure 4 diagrams the ordering by which the three flow fields are brought to simultaneous convergence (see ref. 3.5).

For the nonlinear TSDE, the finite element formulation introduces a variational functional which will be minimized by the first variational principle. Only rectangular elements are used, which allows the potential to be approximated simply by using separation of variables. The finite element formulation is reviewed in Appendix A.

A finite element code was developed for both trilinear and triquadratic elements. The basic shape functions are defined and compared in Appendix B. The trilinear function is continuous (C^0) while the triquadratic spline is slope continuous (C^1). However, the resulting matrix for the quadratic elements has width five along the diagonal, while it is tridiagonal for the linear elements.

III. RESULTS

As described in Ref. 2 and 3.1, the first-order and second-order methods were very successful in a simple supercritical non-lifting case. Table 1 shows a cost and quality comparison. Those results marked by asterisks were judged to show no significant errors due to the far field approximation.

Table 1. Computer Times and Iterations

Box	Far-Field	CP Sec	Sweeps	FO It	SO It
Large	Freestream	*266	612	/	/
Medium	Klunker	114	507	/	/
Medium	FO	*136	597	10	/
Medium	SO	*158	682	12	3
Small	Klunker	34	238	/	/
Small	FO	82	542	10	/
Small	SO	*83	569	11	3
V. small	Klunker	19	171	/	/
V. small	FO	79	524	39	/

*: Error < 0.01 in off-shock C_p and shock location

Refs. 1 and 3.2 describe the extension of these methods to lifting airfoils. Here again both FO and SO methods proved to be of value. The error in circulation of the converged result (as measured against a "standard" result computed with a very

large FD mesh) is plotted in Figure 1 as a function of effort for each matching method. It was also discovered that the accuracy and cost of the results was indpendent of the location of the circulation vortex, an important improvement on the asymptotic methods.

Ref. 3.3 describes the conclusion of the 2D effort. Here the location of the matching boundary was moved to halfway between mesh points, and it was proved that the FO method could converge to good results even with the lower "far field" boundary along the lower surface of an airfoil (Figure 2), as long as this surface was subcritical. The SO method diverged for this case, and showed instability and poor results in other cases where the matching boundary went through a subcritical but rapidly changing area of the flow field.

The 3D FE midfield is now operational and testbed results have been generated. A rectangular wing of $AR = 6$ with constant NACA 0012 section was analyzed by using the FE midfield matching (Figure 5). Table 2 gives the comparison between three cases; large FD box, with no matching, FO matching with panels, and double matching with FE's and panels. In the FE midfield matching, the FD region was reduced to a very small box.

	LARGE BOX	SMALL BOX	VERY SMALL BOX
NUMBER OF MATCHING BOUNDARY	0	1	2
TECHNOLOGY USED	FDM	FDM PANEL	FDM FEM PANEL
OUTER BOUNDARY OF FD BOX	$-15 \le x \le 16$ $0 \le y \le 14.7$ $0 \le z \le 18$	$-.62 \le x \le 1.55$ $0 \le y \le 3.6$ $0 \le z \le 1.88$	$-.15 \le x \le 1.14$ $0 \le y \le 3.6$ $0 \le z \le .91$
FD MESH SIZE (X x Y x Z)	64 x 28 x 20	48 x 18 x 14	42 x 18 x 12
NUMBER OF FD NODES	35840	12096	9072
NUMBER OF FE NODES	0	0	280
NUMBER OF PANELS	0	108	108

TABLE 2 COMPARISONS OF MESH SIZE

Note: Lengths are based on chord = 1

FE and FE fields were iterated alternately for each far field update and the potentials at non-common points on matching boundaries were approximated by Lagrangian interpolation. Figure 6 shows the results when trilinear elements were used and Table 3 demonstrates a further reduction in computational time. The FE midfield matching solution, like the first-order solution, is indistinguishable from the large box solution, while it converged in about 20% less computational time, even though some computational time was used for the Lagrangian interpolations between FD and FE regions.

Stability and convergence of the method were checked by testing several parameters and the following requirements were found. The linearization of the nonlinear term in TSDE should be compatible in FD and FE algorithms. The interface boundary should be at least one node width outside of the supersonic FD area. Lastly, in the FD box we used the customary relaxation factors of 1.5 for elliptic points and .9 for hyperbolic points, but we found that instability resulted from the use of this over-relaxation in FE region when alternate iterations were used.

		LARGE BOX	SMALL BOX	VERY SMALL BOX
CONVERGENCE LIMIT		10^{-5}	10^{-5}	10^{-5}
COMPUTATIONAL TIME (C175 CPU SECS)	TOTAL	749.2	293.0	231.8
	FD	747.7	278.4	175.1
	FE	0	0	31.0
	PANEL	0	13.0	24.8 *
NUMBER OF ITERATIONS	FD	440	470	389
	FE	0	0	389
	PANEL	0	25	25

TABLE 3 COMPARISONS OF COMPUTATIONAL TIME AND NUMBER OF ITERATIONS

*Inefficient matrix solver used.

IV. CONCLUSIONS

The first-order method of far-field matching, whereby the boundary conditions at infinity for a transonic flow problem with subsonic freestream are applied using linear panel methods in the far field, is a success both in 2D and in 3D. It allows comparatively small finite difference meshes to be used without fear of "wind-tunnel-wall-like" far field errors, resulting in cost savings and increased confidence. (An estimate for the far field error is easily computed, as explained in ref. 1.).

The second order method, successful in some of the simpler 2D cases, is touchy and cannot easily be extended to 3D. Its alternative, the finite element mid-field, appears to be stable and accurate, and is likely to yield cost advantages over the first order method.

The first order method is not hard to code and should see immediate application, not only in transonic small disturbance equation codes, but also in other similar problems like full potential equation codes and even separated-variable unsteady flows (Helmholtz-like equations). The finite element midfield, being more complex to code and yielding less advantage, will probably still find its way into the mature forms of these codes - a 20% saving ought not to be scorned in a high intensity production use environment.

APPENDIX A FINITE ELEMENT FORMULATION

The Guderley-von Karman transonic small disturbance equation, (1) is solved in the finite element midfield as well as in the finite difference box inside.

In this study, the finite element formulation is applied only to an elliptic field and an iterative process is used. For a given Dirichlet condition, the calculus of variations introduces a variational functional

$$\mathcal{X}(\phi) = \iiint_{\Omega} \left(K\phi_x^2 + \frac{2}{3} K_\gamma \phi_x^3 + \phi_y^2 + \phi_z^2 \right) dx\, dy\, dz \tag{4}$$

whose first variation yields the TSDE. That is, a function which minimizes the functional is the solution to the Eq.(1). For non-Dirichlet (Eq. 4) type boundary conditions, a surface integral term must be added to Eq. (4). In enforcing normal derivative continuity, it proved to be more convenient to update the solution at the boundary iteratively, when an iterative process is used, than to add this term.

For the finite element approximation, a functional representation is used for the approximate solution such as

$$\phi(x,y,z) = \sum c_i \psi_i(x,y,z) = [\psi_i]\{c_i\}, \tag{5}$$

where the ψ_i's are the basic shape functions, already defined, and c_i's are the coefficients to be estimated. Since only rectangular elements are used in this study, a factorization can be used for simplicity:

$$\phi(x,y,z) = \sum c_{ijk} f_i(x) g_j(y) h_k(z) \tag{6}$$

Then, from Eq. (4) and the first variational principle

$$\delta\mathcal{X} = \partial\mathcal{X}/\partial[c_i] = 0, \tag{7}$$

the discretized finite element algorithm is derived by substitution. However, the resulting FE formulation becomes nonlinear due to the second term in the RHS of Eq. (4). As in the finite difference algorithm, the nonlinear term was linearized and updated iteratively. Hence, Eq. (4) becomes

$$\mathcal{X}(\phi) = \iiint_{\Omega} \left(K - K_\gamma [\phi_x]_e^{n-1}\right)[\phi_x^2]^n + [\phi_y^2]^n + [\phi_z^2]^n \, dx\, dy\, dz,$$

where superscript n stands for n-th iterate and subscript e is the local element in which the velocity is evaluated. It can be shown that this variational finite element algorithm in the purely elliptic field yields precisely the same finite element equation as the Galerkin approach in which the shape function itself is used for the weighting function.

APPENDIX B

Basic Shape Functions in the FE Formulation

Only the one dimensional case is shown in this appendix since the 3D shape functions are factorized in the rectangular element. From Eq. (5), the approximate solution is defined by

$$\phi(x) = \sum c_i f_i(x) = [f_i]\{c_i\}. \tag{8}$$

If we define the basic shape functions in each element ($i = 1, \ldots, I$) as shown in Figure 7, we have

$$\phi(x) = [f_{i-1}^{+} \quad f_i^{-}] \begin{Bmatrix} c_{i-1} \\ c_i \end{Bmatrix} \quad \text{for} \quad x_{i-1} \le x \le x_i$$

in a linear element and

$$\phi(x) = [f_{i-1}^{+} \quad f_i^{o} \quad f_{i+1}^{-}] \begin{Bmatrix} c_{i-1} \\ c_i \\ c_{i+1} \end{Bmatrix} \quad \text{for} \quad x_{i-1} \le x \le x_i$$

in a quadratic element.

Fig. 8 shows the difference in approximating a curve with these respective elements. A *linear element is an approximation of* c_i's which gives $c_i = \phi_i$ ($i = 1, \ldots, I$) but linear variation in each element. Hence it is C^0 continuous.

The quadratic element gives better approximation to a smooth function at interior points of the domain and guarantees C^1 continuity since the derivative of f_i is continuous everywhere.

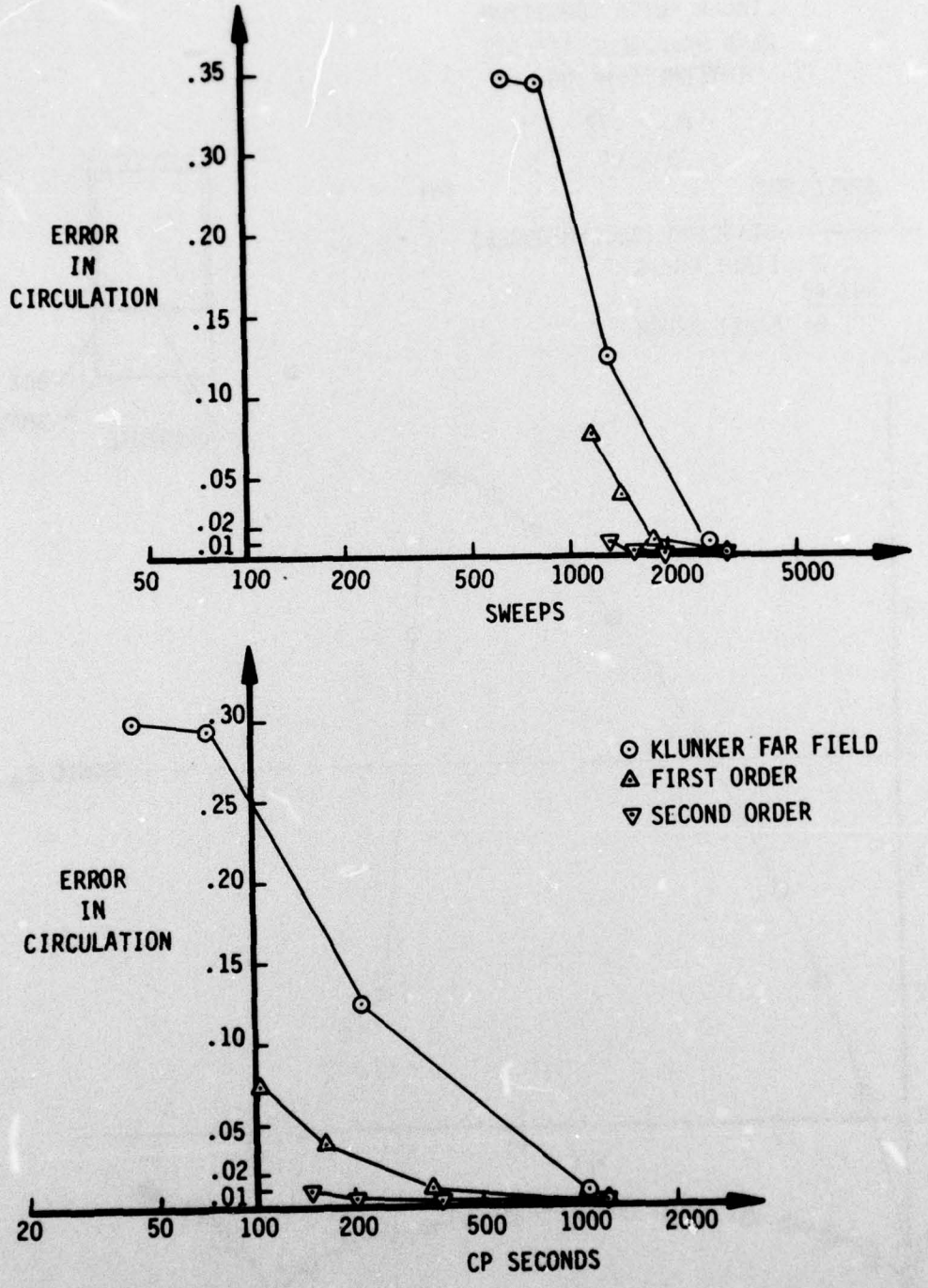

FIGURE 1 ERROR AS FUNCTION OF EFFORT

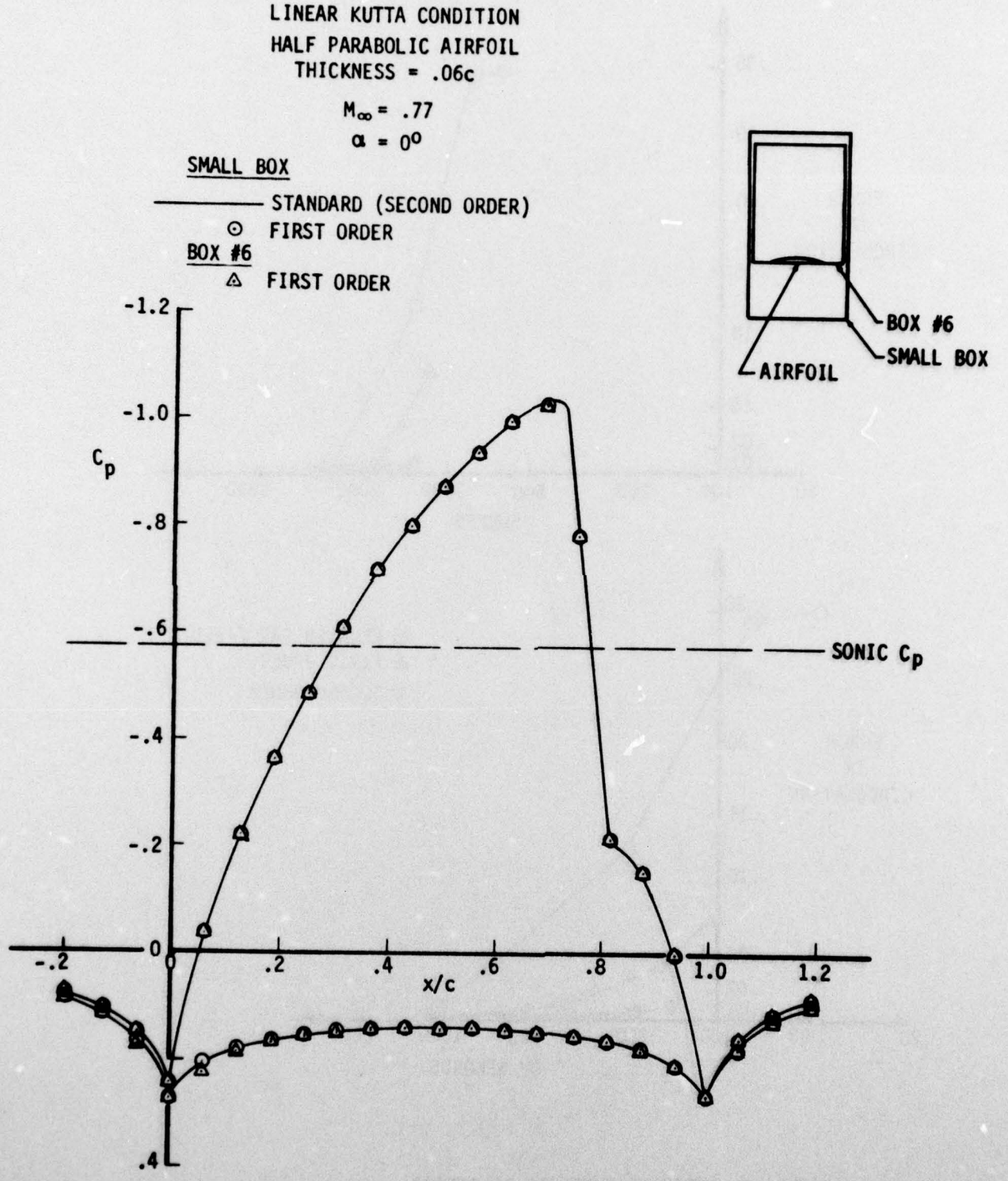

FIGURE 2 BOUNDARY MEETS LOWER SURFACE OF AIRFOIL IN MIXED FLOW

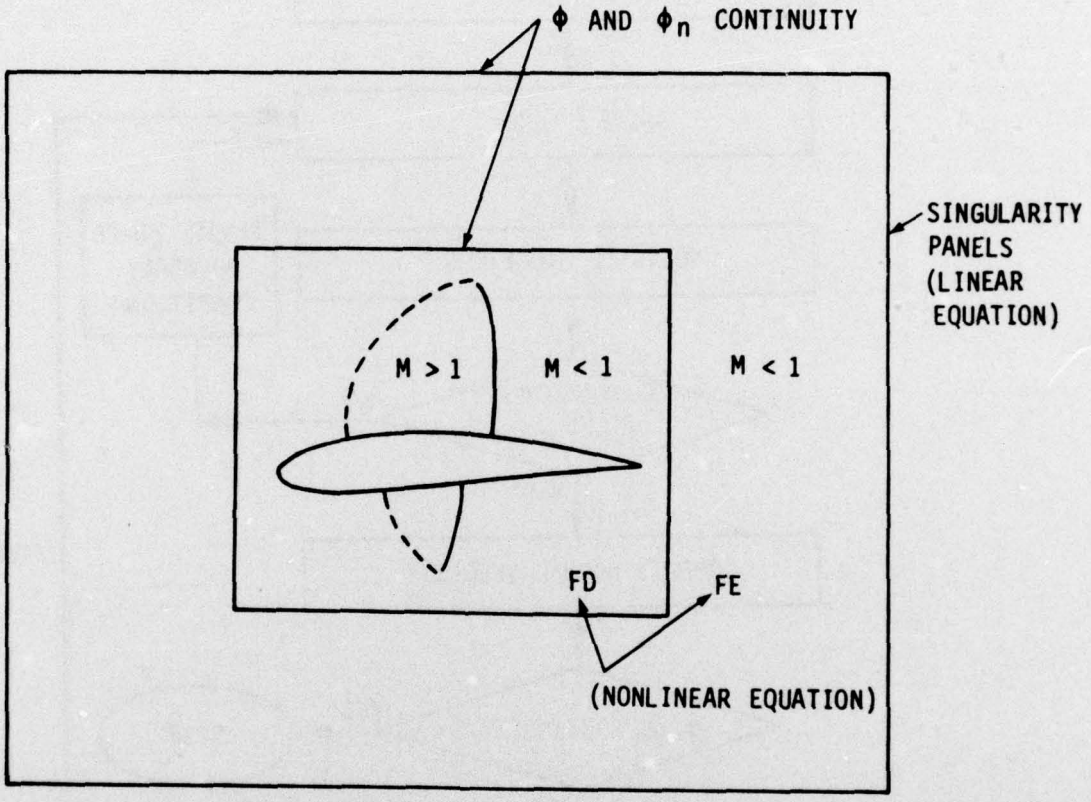

FIGURE 3 FE MIDFIELD MATCHING

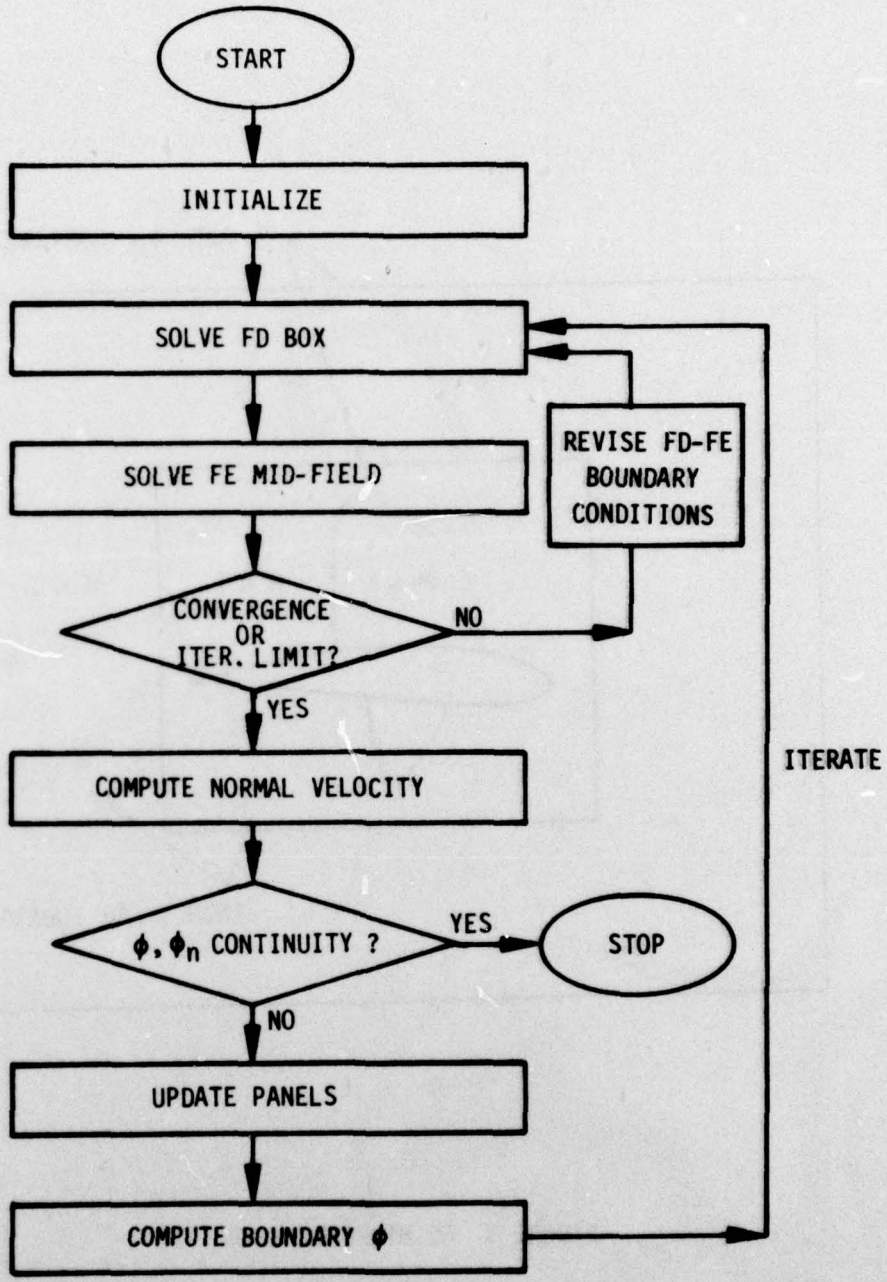

FIG. 4 FLOW CHART FOR THE FAR-FIELD MATCHING

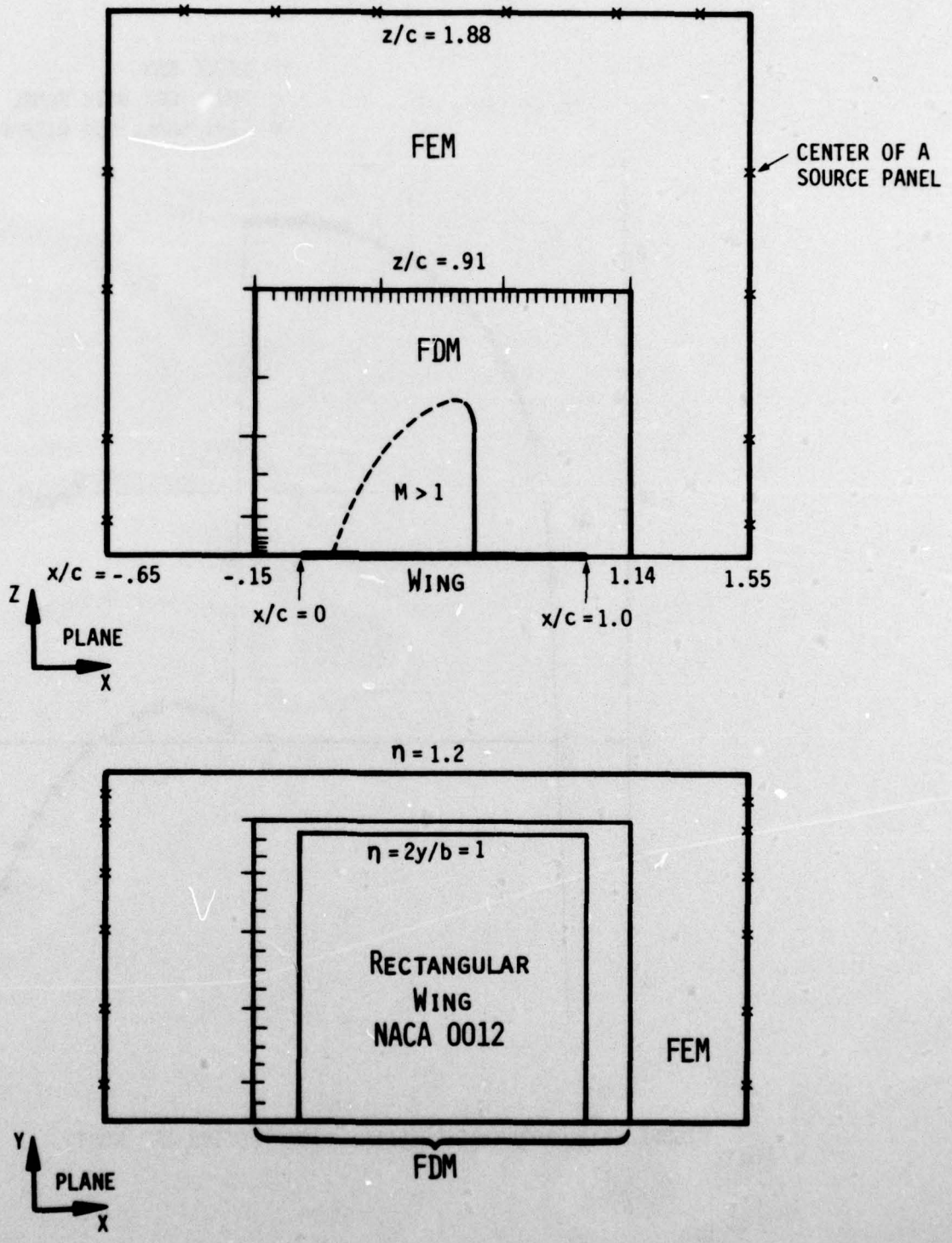

FIG. 5 EXAMPLE OF 3-D MID-FIELD WITH FINITE ELEMENTS

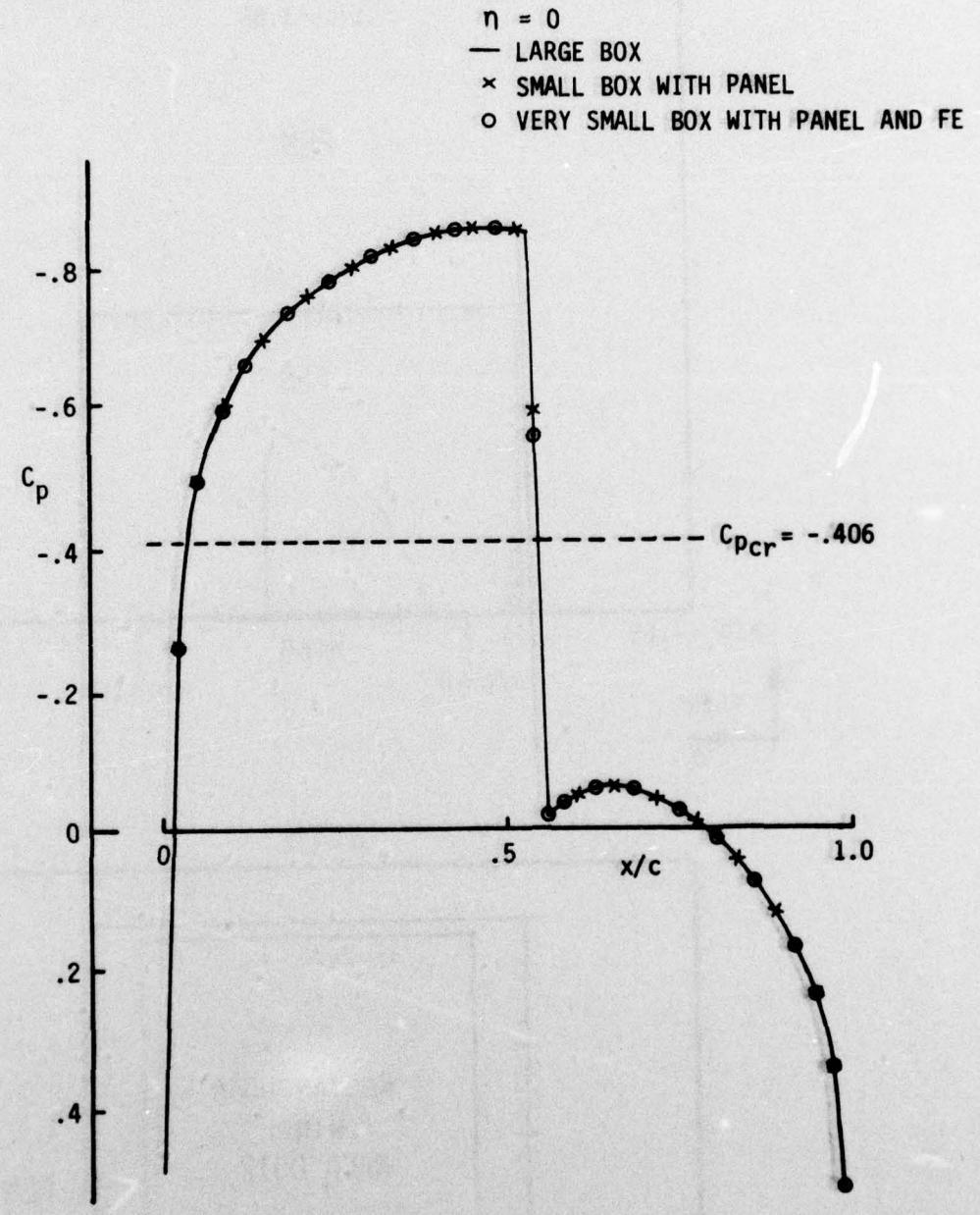

FIGURE 6A CHORDWISE PRESSURE DISTRIBUTION (AT ROOT)

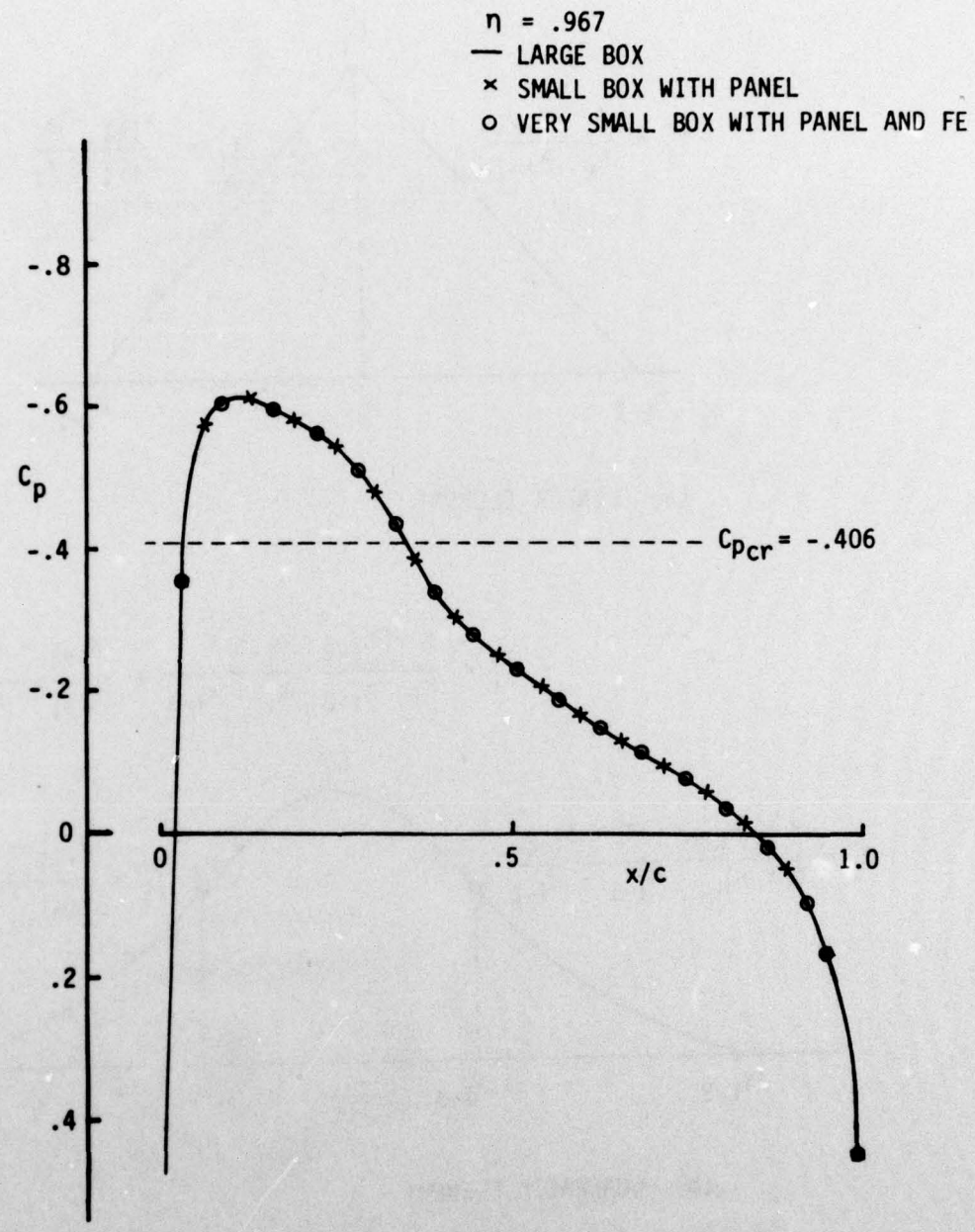

FIGURE 6B CHORDWISE PRESSURE DISTRIBUTION (NEAR TIP)

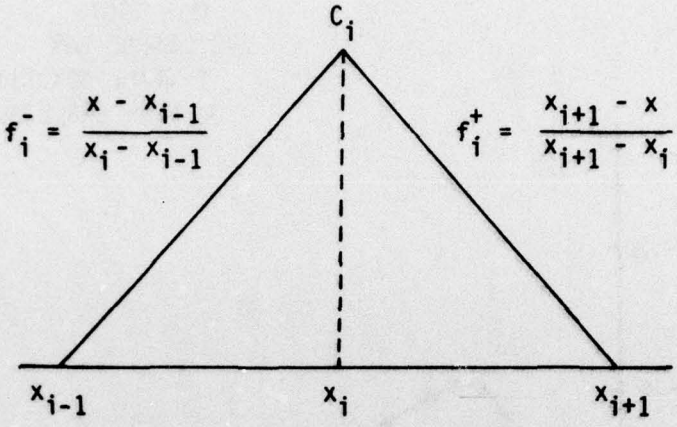

(a) LINEAR ELEMENT

$$f_i^o = \frac{x - x_{i-2}}{x_i - x_{i-2}} \frac{x_i - x}{x_i - x_{i-1}} + \frac{x_{i+1} - x}{x_{i+1} - x_{i-1}} \frac{x - x_{i-1}}{x_i - x_{i-1}}$$

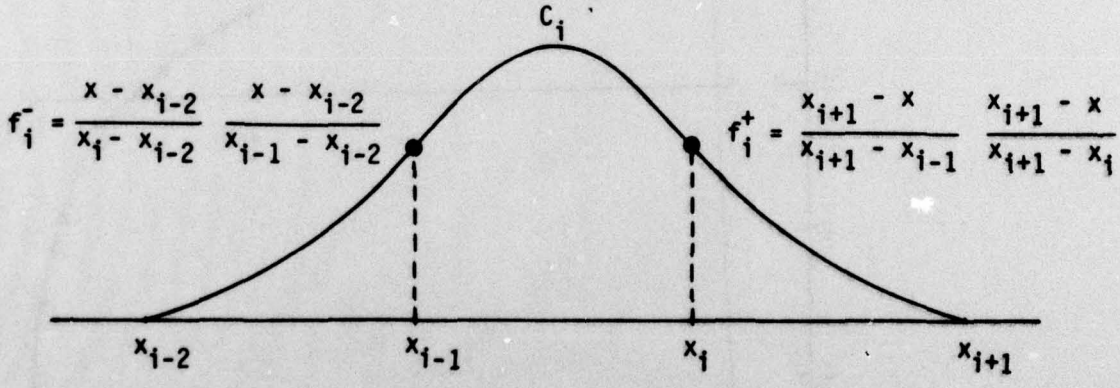

(b) QUADRATIC ELEMENT

FIGURE 7 SHAPE FUNCTIONS IN ONE-DIMENSIONAL ELEMENTS.
($i = 1,\ldots,I$; $x_0 = x_1$, $x_{I+1} = x_I$)

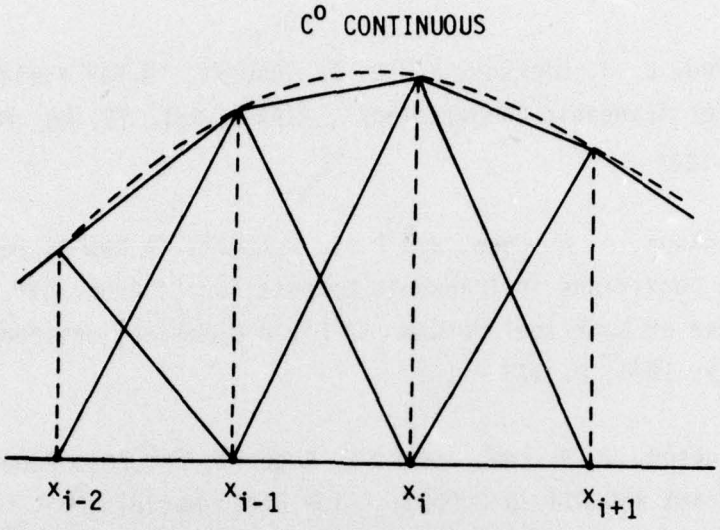

(a) LINEAR SPLINE

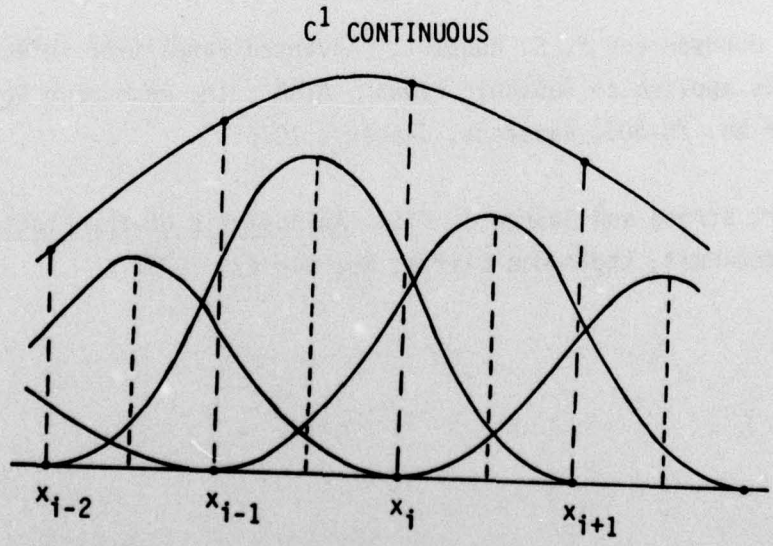

(b) QUADRATIC SPLINE

FIGURE 8 COMPARISON OF LINEAR AND QUADRATIC ELEMENTS

REFERENCES

(1) A. W. Chen, L. J. Dickson, and P. E. Rubbert, "A Far Field Matching Method for Transonic Computations", AIAA J. Vol. 15, No. 10, Oct. 1977, pp 1491-1497.

(2) L. J. Dickson, A. W. Chen, and P. E. Rubbert, "A New Approach to Far-Field Boundary Conditions in Transonic Computations", Proc. 5th. International Conference on Numerical Methods in Fluid Dynamics, Enschede (Netherlands), June-July, 1976, p. 173 - 178.

(3) L. J. Dickson, K. D. Lee, and P. E. Rubbert, Progress Reports, ONR Contract #N00014-76-C-0931, "Flow Field Matching":
(3.1) Period ending August 15, 1976
(3.2) Period ending November 15, 1976
(3.3) Period ending February 15, 1977
(3.4) Period ending May 15, 1977
(3.5) Period ending August 15, 1977.

(4) F. T. Johnson and P. E. Rubbert, "Advanced Panel-type Influence Coefficient Methods applied to Subsonic Flows", AIAA 13th. Aerospace Sciences Meeting (Paper No. 75-50), Pasadena, January, 1975.

(5) Gilbert Strang and George J. Fix: An Analysis of the Finite Element Method. Prentice-Hall, Englewood Cliffs, New Jersey, 1973.

Symbol	Abbreviations, Symbols and Acronyms Meaning
C^n	Continuous to *n*-th order
C_p	Coefficient of pressure
CP	Central Processor
C175	CDC Cyber 175 Computer
D	Dimensions, Dimensional
FD	Finite Difference
FE	Finite Element
FO	First Order
It	Iterations
M_∞	Freestream Mach Number
SO	Second Order
TSDE	Transonic Small Disturbance Equation
ϕ	Velocity Potential
ψ	Second Order Correction to Far Field Potential
AR	Aspect Ratio